Version of Record: https://www.sciencedirect.com/science/article/pii/S0360319924017397
Manuscript_dd714ea525ea90162b251d19d71fb6b3

Surface Exsolving Perovskite Ceramics as Catalyst for Microwave Methane Pyrolysis to co-Generate Hydrogen and Carbon Nanotube

Angela Deibel,[1#] Sonit Balyan,[2#] Xinyuan Zhu,[1#] Changle Jiang,[2] Wenyuan Li,[2] Jianli Hu,[2*] Xingbo Liu[1*]

[1]Department of Mechanical and Aerospace Engineering, West Virginia University, Morgantown West Virginia 26506, United States

[2]Department of Chemical and Biomedical Engineering, West Virginia University, Morgantown West Virginia 26506, United States

Abstract

In this study, we have successfully developed a novel surface exsolving perovskite ceramic, which demonstrates the ability to simultaneously generate CO_x-free hydrogen and carbon nanotubes (CNTs) through methane pyrolysis under the influence of microwave irradiation. We conducted an extensive survey and optimization of various perovskite materials specifically tailored for microwave applications. Among the materials investigated, nickel-doped strontium titanium oxide (STON) emerged as the most promising candidate, exhibiting both a satisfactory methane conversion rate and excellent responsiveness to microwave irradiation. Refinement of STON was carried out by fine-tuning the Ni content, optimizing the reduction dwell time, and adjusting the reduction temperature. Notably, $SrTiNi_{0.08}O_3$ (STON8), demonstrated an impressive initial methane conversion rate of up to 40%. Transmission Electron Microscopy (TEM) provided visual evidence of the correlation between Ni content and reduction temperature, with respect to the exsolved Ni metal particle size. This finding highlights the immense potential of surface exsolving perovskite ceramics as a highly effective catalyst for the simultaneous production of CNTs and COx-free hydrogen via methane pyrolysis under microwave irradiation. It represents a step forward in the field of catalytic materials and microwave-driven processes.

Keyword: Methane pyrolysis, microwave excitation, turquoise hydrogen, carbon nanotube, perovskite catalyst, surface exsolution

---

Angela Deibel, Sonit Balyan and Xinyuan Zhu contribute equally to this study
* corresponding authors: John.hu@mail.wvu.edu, Xingbo.liu@mail.wvu.edu

© 2024 published by Elsevier. This manuscript is made available under the Elsevier user license
https://www.elsevier.com/open-access/userlicense/1.0/

1. Introduction

Methane pyrolysis represents a compelling utilization of natural gas due to its dual benefits. By decomposing methane into its elemental components, hydrogen and carbon, this process offers a sustainable pathway for energy and materials production. Moreover, this approach mitigates greenhouse gas emissions, as it avoids the release of carbon dioxide associated with traditional natural gas utilization methods such as combustion. Overall, methane pyrolysis presents a versatile and environmentally friendly strategy for maximizing the value of natural gas resources while contributing to efforts towards a low-carbon future. An innovative one-step, in-field conversion process can effectively utilize unutilized methane from flare gas to produce hydrogen and carbon nanotubes (CNTs). This near-zero CO_2 process presents an appealing commercial deployment option, especially in utilizing fossil resources. Hydrogen, a clean and sought-after fuel, is witnessing increasing demand as global leaders strive to combat greenhouse gas (GHG) emissions. On the other hand, CNTs are highly esteemed for their diverse applications and remarkable material properties, including high strength, flexibility, ionic and electronic conductivity, as well as lightweight.[1-13]

Traditionally, CH_4 undergoes cracking at high temperatures (500-700°C) using a catalyst, and the resulting carbon deposits on the surface of metal catalyst nanoparticles, accumulating there until they grow into CNTs. State-of-the-art CNT-producing materials, such as Ni/SiO_2 and $Ni-Cu/SiO_2$,[14] have demonstrated methane conversion rates exceeding 70%. Other commonly used materials include Ni/Al_2O_3,[15] Ni/TiO_2,[16] or Ni/MgO.[17] The extensive exploration of nickel catalysts and many others can be attributed to their cost-effectiveness and affinity for methane cracking.[18-20]

An emerging alternative to conventional thermal cracking involves microwave excitation. This approach has shown significant improvements in catalysis and material processing efficiency across various applications. Microwave irradiation offers several advantages over traditional thermal methods. It rapidly transfers energy through an electromagnetic field, simultaneously heating the material's volume at a molecular level. In contrast, convective heating relies on heat transfer from the outside-in.[21] The selective heating capabilities of microwave excitation enable a reduction in the overall operation temperature without compromising catalytic

activity. This is achieved through accelerated reaction rates at active sites, resulting from the increased temperatures experienced by metal catalyst nanoparticles compared to the bulk supporting material.[22, 23] While measuring the temperature difference between bulk operation and catalyst site temperature remains challenging with microwave excitation, research on the decomposition of hydrogen sulfide (H_2S) using a MoS_2 catalyst on an Al_2O_3 support has demonstrated a minimum increase of 200°C at active sites.[24] This was characterized by a significant phase-change in Al_2O_3 support materials after microwave reactions. Microwave heating offers attractive benefits, including energy savings from reduced process times,[24] lower overall operation temperatures,[25, 26] and accelerated catalytic activity,[22] making it an appealing method for methane pyrolysis.

The existing literature on microwave methane pyrolysis catalysts with CNT generation capabilities is limited, highlighting a significant research gap. Some studies have explored different catalyst materials and reported varying degrees of success in CNT production and methane conversion rates. Zeng et al.[27] achieved CNT growth using a carbon/carbon (C/C) composite which grew CNTs 20-200nm in diameter. But they did not provide data on the corresponding methane conversion rate, leaving an incomplete understanding of the catalyst's performance. Dominguez et al.[28] used activated carbon as a catalyst and observed high initial conversion rates ranging from ~100% to 49%, which decreased to ~29% to 7% within 90 minutes. Fidalgo et al.[29] reported on microwave-assisted methane decomposition using various catalysts, including Fe-doped carbon fiber, Ni-doped carbon fiber, and activated carbon. Although they observed the formation of carbon nanofilaments through multiple scanning electron microscope (SEM) images, they did not provide specific methane conversion data, leaving questions about the catalysts' overall effectiveness. In our previous work, we demonstrated methane catalytic pyrolysis by microwave on Ni-Cu catalyst supported on CNT, showing a highly efficient conversion process and a casted low cost of \$1/kg H_2 production.[30] Although exciting progress is being made on these carbon-based catalysts, technical barrier remains in these carbon-based catalysts for large-scale application, e.g. sacrificial use of the catalyst, difficulty to separate metal catalyst residual from the CNT product, and the use of precious metals for high conversion rate.

In contrast, a new strategy could be to use ceramic catalysts for CNT production under microwave (MW). There are many underlying advantages associated with the ceramic-based catalyst system: (1) unlike carbon-based catalysts, they can be recycled from the produced CNT for repeated use to lower the operation cost, (2) ceramics have strong mechanical and electronic substrate-catalyst interaction, which could prevent the deactivation of the loaded catalyst, (3) ceramics have high resistance to high-temperature aging, therefore allowing for long-lasting service time, (4) ceramics have a wide range of tunable electronic/dielectronic properties that can be mediated for high efficient application in the microwave, and lastly (5) most ceramics are cheap, whose large scale manufacture in industry is widely available compared to the carbon-based catalysts.

In this study, as an extension of our previous study on CNT-based catalysts,[30] a set of ceramic materials with different physic properties are investigated for the first time in the microwave methane conversion to extend the catalyst to the ceramic region. Of them, an A-site deficient perovskite material, strontium titanium nickel oxide (STON), is proven most effective. This material was tuned to produce optimal Ni particle size through surface exsolution strategy (precipitation of Ni metal particles on the surface of STON trigger by reduction of the A/B site unbalanced perovskite, different from traditional physically dispersed catalyst particle on the substrate) for microwave absorption, methane cracking, and CNT generation. TEM analysis on the effect of reduction temperature and Ni-doping amount on exsolved particle size is presented.

This work extends the horizon of catalyst materials by introducing ceramic catalysts, exemplified by the remarkable effectiveness of strontium titanium nickel oxide in microwave methane conversion. By optimizing Ni particle size and methane cracking, STON demonstrates remarkable efficiency in CNT generation. These finding along with microwave pyrolysis' intrinsic advantages such as rapid heating, and precise control over reactions, scalability and reduced environmental impact showcase transformative potential of ceramic catalysts in the realm of microwave-assisted pyrolysis.

2. Methodology

2.1 Fabrication of Exsolution Catalysts

All catalysts were prepared by solid-state reactions. Take STON for an example, stoichiometric amounts of $SrCO_3$ (Alfa Aesar), NiO (Sigma Aldrich), and TiO_2 (Alfa Aesar) were ball-milled for 24 hours before being pressed into pellets and calcined in air at 1200°C for 5 hr. After calcination, all samples were confirmed by X-ray diffraction (XRD) to ensure that a pure phase was achieved. The sample was then mixed with 10wt.% starch and 3wt% PVB binder pressed into pellets before reduction. The starch was burned out in a tube furnace in flowing air to create pores inside the pellets at 500°C before continuing to the reduction temperature. After purging with N_2 the samples dwelled in pure H_2. The target temperatures (600°C, 700°C, 800°C, 900°C) and dwell times varied per reduction method (RM) chosen (note, if not reduced first, catalysts are not able to effectively catalyze methane pyrolysis). The ramp rate is 5°C/min. Catalysts reduced in H_2 at 800°C for 12 h were washed by excessive 0.5M HNO_3 overnight. The resultant solutions were collected and examined by inductively coupled plasma optical emission spectrometry (ICP-OES) for element analysis.

2.2 Testing Conditions in Microwave Reactor

After reduction, pellets were reground to powders in a mortar, and 1.5 g of catalyst was tested in a fixed-bed microwave reactor (MC1330, Lambda Technologies Inc., Morrisville, NC, United States), operating at 5.85GHz. Gas mixture of testing was N_2 and CH_4, the flow rates of which were 21 mL/min and 9 mL/min, respectively. Not all samples tested during the preliminary screening of materials were able to be heated under microwave conditions. These materials were physically mixed with 10 wt.% silicon carbide (SiC) to enable microwave heating to see if operation temperatures were achievable. The microwave reactor has a temperature controller module that allows the catalyst to reach programmed temperatures.

For all samples tested under conventional heating conditions, a tube furnace (Series 2404 controller, Applied Test System, Butler, PA, United States) was used. The same reaction and amount of catalyst were investigated in the tube furnace reactor to compare with experiments taking place in the microwave reactor. The testing parameters of flow rates and reaction temperatures remained the same as under microwave.

Conversion data of methane to hydrogen was measured by micro gas chromatography (Micro GC 3000A, Agilent Technologies, Santa Clara, CA, United States). Nitrogen was introduced in the testing system as an inert and internal marker for methane conversion calculation only. The methane conversion was calculated using Equation 1:

$$X_{CH_4} = \left[1 - \frac{F_{in-N_2} \times C_{out-CH_4}}{C_{out-N_2} \times F_{in-CH_4}}\right] \times 100\% \quad (1)$$

where, X_{CH_4} refers to the methane conversion,
F_{in-N_2} refers to the flow rate of inlet nitrogen,
C_{out-CH_4} refers to the concentration of outlet methane detected by Micro-GC,
C_{out-N_2} refers to the concentration of the outlet nitrogen detected by Micro-GC
F_{in-CH_4} refers to the flow rate of inlet methane

2.3 Materials Characterization

Prepared sample phases were confirmed through XRD (PANalytical X'Pert Pro X-ray Diffractometer) before testing. The XRD operated at 45 kV with a current of 40 mA, a step width of 0.0167°, and a scanning rate of 0.1078 seconds per step, from the start angle of 20° and an ending angle of 110°. A scanning electron microscope (Hitachi S-4700 SEM) was used to analyze the surface morphology of the as-prepared samples before reduction. All powder samples were mixed with a small amount of ethanol and mounted on a silicon wafer using a pipet, then dried before SEM analysis. Reduced and spent samples after microwave testing were characterized with a Transmission Electron Microscope (TEM) (JEOL JEM-2100) upon a Silicon Monoxide Type-A 300 Copper mesh grid (Ted Pella, INC). Raman spectra was obtained from 1000 to 2000 cm^{-1} using a Raman spectrometer (Renishaw inVia Raman microscope, excitation at 532 nm).

3. Results and discussion

3.1 Screening of Catalysts for Microwave Reactor

Ceramics of different structures and properties, such as perovskites and fluorites, have been explored in this work to understand their behavior under MW. The unique features of tested materials and the response to MW are summarized in Table 1. Important properties for application in MW include high dielectric constant, or semi-conducting joule heating nature upon MW irradiation, stability upon exposure to methane and hydrogen, and cost-

effectiveness. Therefore, the criteria to screen the catalyst candidates for the continuation of the study are responsiveness to microwave irradiation, methane conversion rate, and general cost of the catalyst.

Out of all the materials examined in Table 1, the Strontium Titanium Nickel Oxide (STON) material system best met microwave absorption requirements with acceptable methane conversion rates and CNT generation capability, and therefore was chosen for further investigation.

Table 1. Catalyst candidates screened for Microwave Heating Response

Composition	Microwave Heating Response	Potentially Desirable Material Characteristics	Drawbacks
$Y_{0.8}Ca_{0.2}Cr_{0.9}Co_{0.2}O_3$	heat without assistance	Appropriate semi-conducting abilities and stability in reducing atmospheres	No methane conversion.
$Y_{0.8}Ca_{0.2}Cr_{0.9}Ni_{0.1}O_3$	heat without assistance	Appropriate semi-conducting abilities and stability in reducing atmospheres	No methane conversion.
$CaMnO_3$	heat without assistance	Appropriate semi-conducting abilities and stability in reducing atmospheres	Low methane conversion (<15%)
$CaAl_{0.2}Mn_{0.8}Ni_{0.3}O_3$	Unable to heat	Appropriate semi-conducting abilities and stability in reducing atmospheres	Unable to heat.
$CaMnNi_{0.3}O_3$	Unable to heat	Appropriate semi-conducting abilities and stability in reducing atmospheres	Unable to heat.
$Gd_{0.1}Ce_{0.9}Ni_{0.02}O_2$	heat without assistance	Great chemical compatibility with Ni and stability towards CH_4 and H_2	Showed very fast, clear degradation.
$Gd_{0.1}Ce_{0.9}O_2$ -Ni physically mixed in at 2wt%, 4wt%, & 6wt%	heat without assistance	Great chemical compatibility with Ni and stability towards CH_4 and H_2	Showed very fast, clear degradation.
$(Y_2O_3)_{0.08}(ZrO_2)_{0.92}$	heat without assistance	Great chemical compatibility with Ni and stability towards CH_4 and H_2	Stable, but low methane conversion (<10%).
$SrTi_{0.95}O_3$ (STO)	Unable to heat	Cost effective, stability in reducing atmospheres	Unable to heat by microwave.
$SrTiNi_{0.12}O_3$	heat without assistance	Cost effective, Ability to exsolve metal particles	No clear drawback.
$BaTiNi_{0.12}O_3$	heat without assistance	Barium samples were created with a hyper-stoichiometry of Ni at the B-site to promote metal particles exsolution	Fast degradation.
$Ba_{0.5}Sr_{0.5}TiNi_{0.12}O_3$	heat without assistance	Barium samples were created with a hyper-stoichiometry of Ni at the B-site to promote metal particles exsolution	Good conversion, but with faster degradation.
$La_{0.1}Sr_{0.9}TiNi_{0.1}O_3$	heat without assistance	Lanthanum was added to the STO material system due to its high valence, which can help facilitate the exsolution process	Phase purity hard to achieve in sample.
$Sr_{0.81}Y_{0.072}Ti_{0.95}Ni_{0.12}O_3$	heat without assistance	Yttrium is a known microwave absorber, added to STON system to promote heating	Phase purity hard to achieve in sample.
$SrTi_{0.95}O_3$ - Ni infiltrated @ 1.7wt%, 3wt% & 20wt%	Ni-doped at 1.7wt% heat up, all other runs needed 10wt% SiC to achieve heating. Sintering and difficulty heating occurred in consistently in 3wt% and 20wt%.	Infiltrated samples created to compare to exsolution samples.	Unstable heating response, low methane conversion.
$SrTi_{0.95}O_3$ - Cu infiltrated @ 1.7wt% & 3wt%	Unable to heat without 10wt% SiC.	Infiltrated samples created to compare to exsolution samples.	Low methane conversion.
$SrTi_{0.95}O_3$ – Pd infiltrated @ 1.7wt% & 3wt%	Unable to heat without 10wt% SiC.	Infiltrated samples created to compare to exsolution samples.	High-cost of materials.

3.2 Effect of Reduction on Catalytic Conversion of Methane

We adopted an exsolution method to finely tune the properties of STON. The ability to exsolve a catalyst stems from the unique characteristics of the perovskite oxide structure. A perovskite oxide material usually consists of the general formula ABO_3, with the B-site usually occupied by transition metals. Both the A-site and B-site can be substituted by one or more foreign elements to control the stoichiometry of the perovskites. A-site deficiencies can also be utilized to promote the exsolution process through the electroneutrality principle. During the reduction process, a singular metal ion will have connecting oxygen atoms removed, separating it from the perovskite structure. Then, the metal ion will migrate and nucleate to the surface to form small nanoparticles with other metal ions experiencing the same situation.[31] Controlling the size of the exsolved nanoparticles is critical in CNT growth. The exsolved particle size can be controlled through reduction variables, including temperature, dwell time, composition of gas,[32, 33], and dopant quantities.[34]

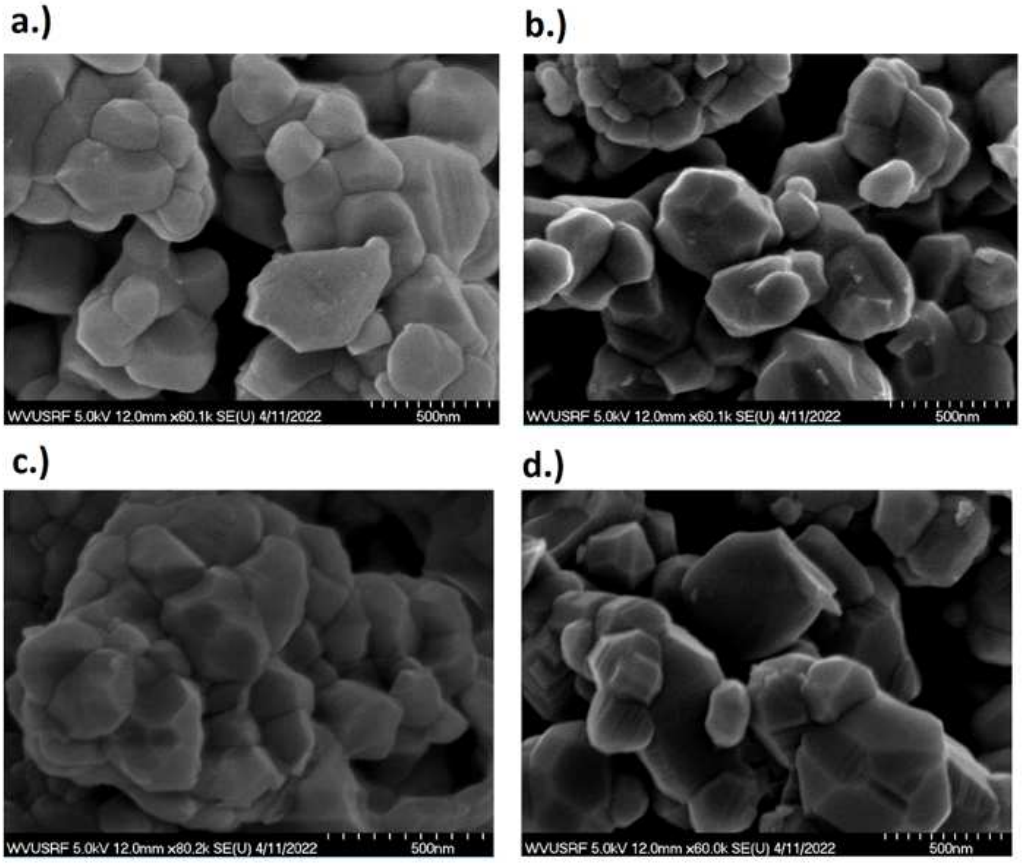

Figure 1. SEM of calcined samples before reduction: a)STON6, b) STON8, c) STON10, and d) STON12.

The first reduction variable studied was the effect of dwell time in the reducing environment at a fixed temperature. STO with different Ni catalyst doping, $Sr(TiNi_{0.06})O_3$ (STON6), $Sr(TiNi_{0.08})O_3$ (STON8), $Sr(TiNi_{0.10})O_3$ (STON10), and $Sr(TiNi_{0.12})O_3$ (STON12), were fabricated then reduced using a twelve-hour dwell (RM600) and a two-hour dwell (RM600-2h) in pure H_2 at 600°C. Figure 1 shows the as-prepared samples with a consistent surface morphology. The Ni doping level does not affect the morphology of these catalysts. Particles with clear facets were observed for all candidates, which is consistent with the properties of $SrTiO_3$ reported elsewhere.[35] The particle size distribution ranges from 300 to 600 nm, with smaller grains clearly visible. These fine particles, possessing a tremendous amount of surface area, could benefit the surface exsolution process in controlling the size of Ni and total area of active for catalytic pyrolysis. For the methane conversion reaction using these catalysts, the input of the reactor was methane with a flow rate of 9 mL/min and nitrogen with a flow rate of 21 mL/min. Catalytic activity was measured through the percentage of methane conversion to confirm the production of CNTs. The methane conversion data are presented in Figure 2. In general, the 12h dwell time produced higher initial methane conversion, with the exception as STON6 which performs better at shorter reduction time. Both of the reduction methods showed degradation along the measurement course.

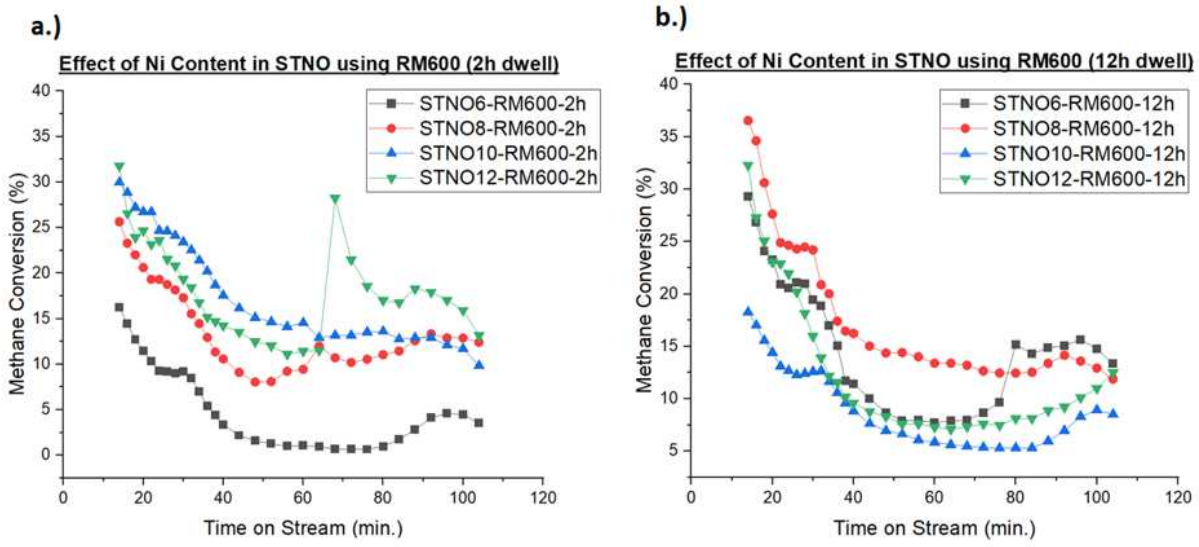

Figure 2. Methane conversion as a function of time on stream. All samples were heated by microwaves to 500°C. The catalytic activity of a.) RM600-2h and b.) RM600 (12h).

A temperature study was followed on STON12 sample, keeping the dwell time fixed at 12h to observe the relationship between particle size and reduction temperature through the range of 600°C-900°C. The reduction methods were named as follows: RM600, RM700, RM800, and RM900. The reduced samples were tested under microwave heating conditions at 500°C. STON12-RM900 sintered on the first run and experienced difficulty in heating, possibly due to the size and distribution of Ni particles on the surface. It is theorized that if too much metal exsolves to the surface, it exhibits bulk Ni metal properties. Bulk Ni metal does not absorb microwaves and instead reflects them. To achieve heating, on the second test of STON12-RM900, 10wt% of SiC was physically mixed with the reduced exsolution catalyst to assist in microwave heating. Methane conversion results are presented in Figure 3. Conversion humps within 100-150 min interval can be observed for these catalysts. Such phenomena are not uncommon in our experiments. We attribute them to the blockage of gas pathways by the produced carbon nanotubes. Initially, 1.5 g of catalyst powders is packed into an 8 mm OD quartz tube with sufficient gas flow channels inside the powders. However, as the reaction progresses, the accumulation of CNTs obstructs these channels inside the packed powders, leading to the actual loss of nearby catalysts due to lack of gas exposure. This buildup causes pressure to increase upstream. Subsequently, when the pressure reaches a threshold to overcome the blockages, gas flow will either gradually or abruptly resume, resulting in a slow recovery or spike in conversion rates, depending on the pressure difference.

and exsolved Ni particles for each temperature imaged by TEM are shown in Figure 4. The average particle size indeed increased with higher reduction temperatures, confirming what has been reported in other literature.[32, 33] RM600, RM700, RM800, and RM900 resulted in average Ni particle sizes around 9-10 nm, 10-12 nm, 10-20 nm, and 20-40 nm, respectively.

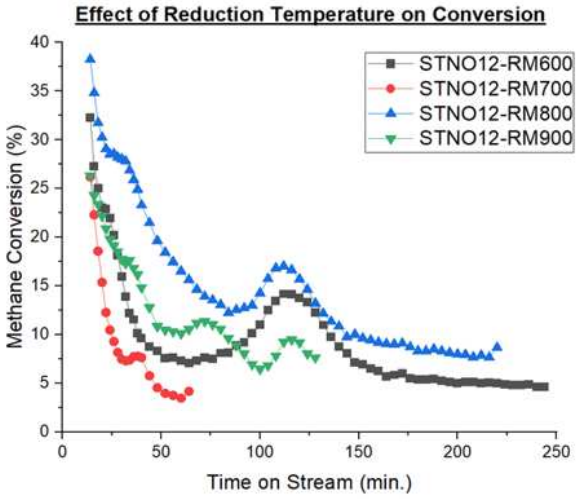

Figure 3. The effect of reduction temperature on catalyst activity. STON12-RM900 was the only sample unable to achieve operation temperature under microwave heating without the addition of 10wt% SiC.

In Fig. 3, STON12-RM800 had the highest methane conversion of any exsolution catalyst tested thus far and produced repeatable results in multiple runs. TEM was carried out on the spent samples and confirmed carbon growth. Produced CNTs from STON12-RM800 are shown in Figure 4 (e, f). The CNTs grown were thick with varying diameters from 100-500 nm, with a bamboo-shoot structure. From the TEM images, the thick CNTs look to be mainly tip-growth.

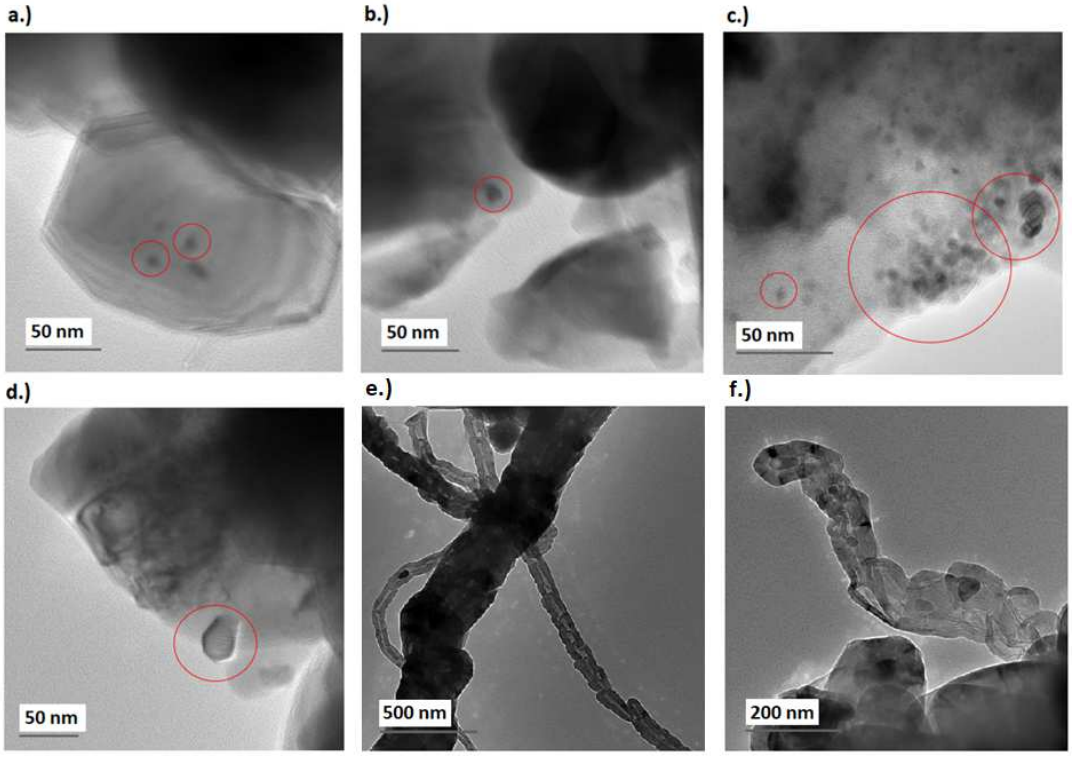

Figure 4. TEM observation of exsolve particle sizes at different reduction temperatures: a.) STON12-RM600, b.) STON12-RM700, c.) STON12-RM800, d.) STON12-RM900. TEM of carbon nanotubes in spent STON12-RM800 after microwave heating to 500°C with an input gas of methane at a flow rate of 9mL/min and nitrogen at a flow rate of 21 mL/min.: e.) & f.).

RM800 appeared as the optimized reduction method based on the methane conversion results and approximate particle size of exsolved Ni. In the referenced study[36, 37], Ni doping level was the main factor used to control particle sizes. Perovskite oxides $LaAl_{1-y}Ni_yO_3$ (y=0,0.5,0.2) were prepared and reduced in a gas mixture of 5 vol % H_2/N_2 at a total flow rate of 30 mL min^{-1}. The bulk material acted as a limited reservoir to pull from, possibly limiting the maximum size of particles exsolved. The final findings in the referenced studies concluded that the Ni particle sizes were almost proportional to Ni content in $Sr_2Fe_{1.5-x}Ni_xMo_{0.5}O_{6-\delta}$ or $LaAl_{1-y}Ni_yO_3$ (y=0,0.5,0.2) [36, 37], and a high dopant level leads to aggregation of exsolved particles to large size. To observe the effect of Ni dopant amount on exsolved particle size, STON 6, 8, 10&12 were all reduced using best-performer RM800. The amount of exsolved Ni metal particles was evaluated using ICP-OES and listed in Table 2. There are 8.6 mg of Ni metal particles exsolved per 1 g of STON6 catalyst after reduction. Additionally, this value is 12 mg/g, 14 mg/g, and 18 mg/g for STON8, STON10, and STON12, respectively. The exsolved amount of Ni is proportional to the doping amount for all samples. The exsolution efficiency (exsolved Ni/doped Ni) is 47.6%, 49.0%, 45.8%, and 48.9% for STON6, STON8, STON10, and STON12, respectively. This confirms an effective and consistent exsolution process in this study.

Table 2 ICP-OES analyses of the amount of exsolved Ni metal particles in different catalysts.

Sample ID	**STON6**	**STON8**	**STON10**	**STON12**
Ni metal/STON	8.6mg/g	12mg/g	14mg/g	18mg/g
Exsolution Efficiency	47.6%	49.0%	45.8%	48.9%

XRD results in Figure 5 indicate that for all samples, NiO was reduced to Ni metal, confirming that Ni metal is the exsolution species in STON.

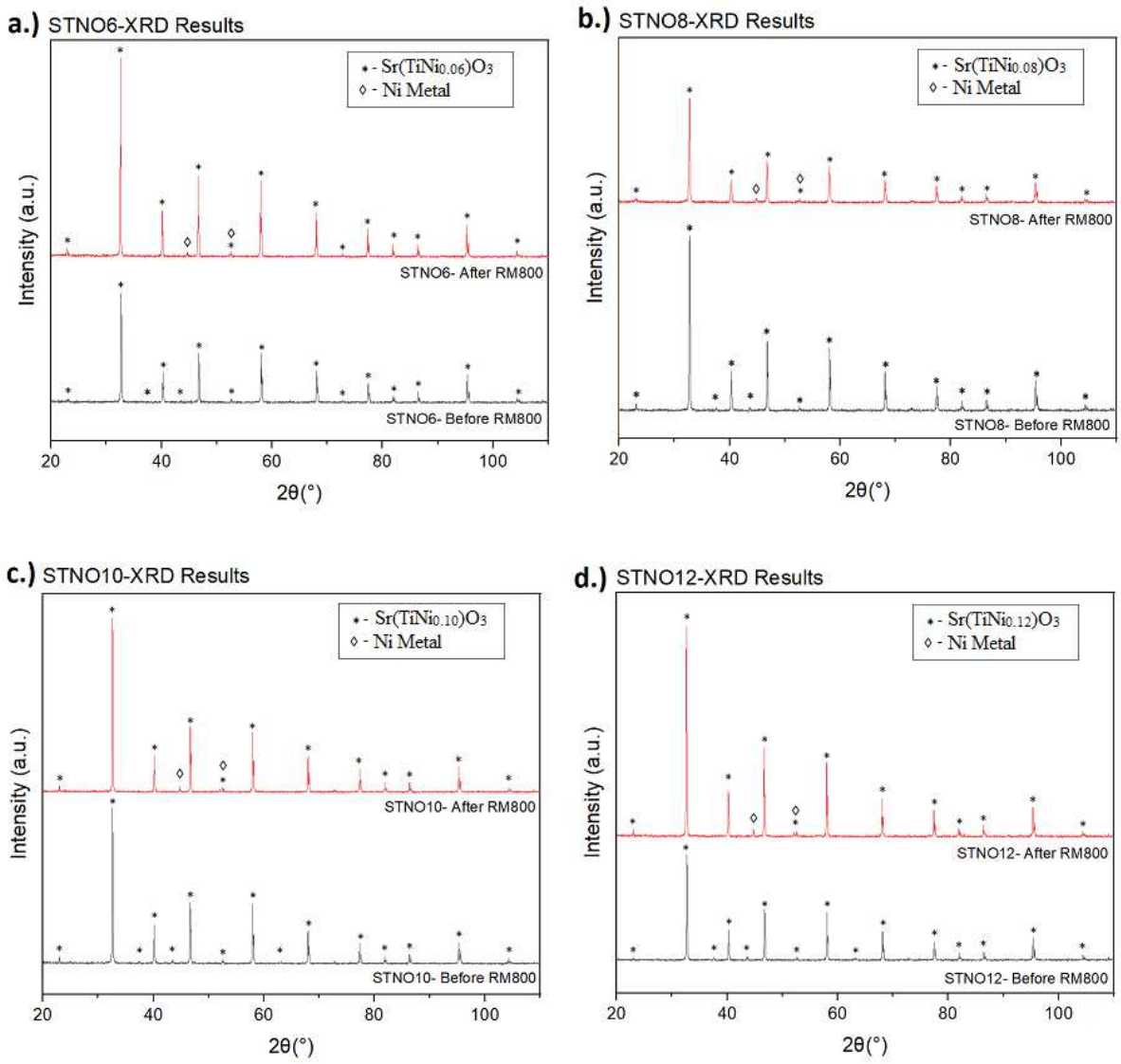

Figure 5. XRD results before and after RM800 of a.) STON6, b.) STON8, c.) STON10, and d.) STON12.

TEM analysis was performed on reduced samples and presented in Figure 6. An average size of ~25 nm was observed for Ni particle sizes in samples STON6-RM800 and STON8-RM800. The biggest difference between these two samples was the increase in the population of exsolved Ni, as STON6-RM800 had very few exsolved particles compared to STON8-RM800. Both had good consistency of Ni particle size throughout the sample, although STON8-RM800 had the appearance of some particles going up to ~75nm. STON10-RM800 and STON12-RM800 both experienced high populations of exsolved particles with a large variation in size ranging from 30nm to 100nm. The majority of these particles for STON10-RM800 and STON12-RM800 fell

between ~30-50nm. The exsolution trend observed was that increasing the content of Ni in the sample increased particle size and population, but the higher doping level such as STON10 and STON12 will likely generate aggregated Ni particles.[37, 38]

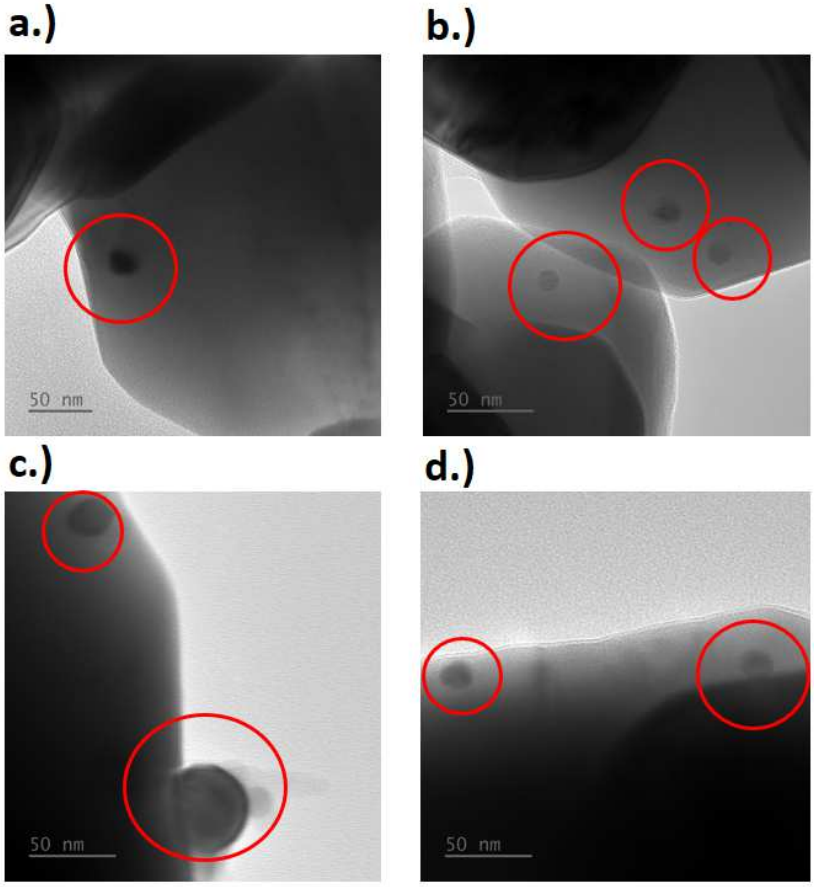

Figure 6. TEM results of exsolved Ni particles in relation to Ni content in sample a.) STON6-RM800, b.) STON8-RM800, c.) STON10-RM800, and d.)STON12-RM800.

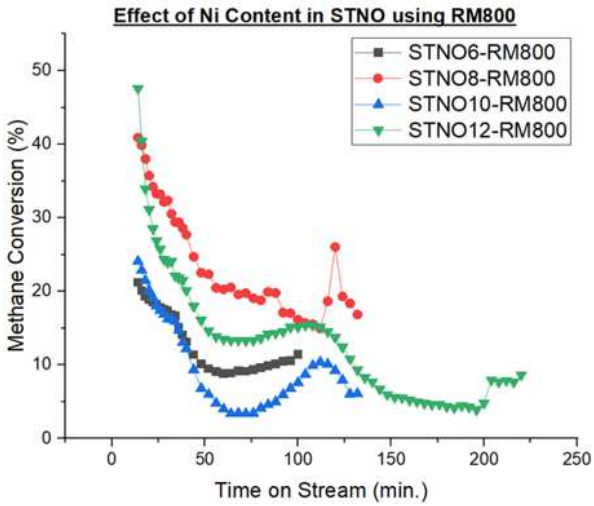

Figure 7. Methane conversion as function of time on stream for samples with different Ni loading reduced by RM800.

Methane conversion results of STON6, 8, 10, and 12 reduced by RM800 are presented in Figure 7. STON8-RM800 and STON12-RM800 had the highest methane conversions, with STON8-RM800 slightly outperforming STON12-RM800 in terms of methane conversion. STON12-RM800 starts around 49% methane conversion then deactivates to ~15% after two hours. STON8-RM800 starts lower around 40% methane conversion then deactivates to ~17% after two hours. In comparison, the state-of-the-art carbon-based catalyst yielded a close conversion rate of ~50% under similar conditions. The main difference between these two STON catalysts is the initial conversion measured and the slightly slower deactivation of STON8-RM800. STON6-RM800 and STON10-RM800 both had poor performance. Re-testing of STON6-800 and STON10-RM800 provided similar results.

Spent STON8-RM800 was selected for TEM analysis due to it being competitive with STON12-RM800. Produced CNTS are shown in Figure 8. In STON8-RM800, some large bamboo-like nanotubes formed, with diameters of around 100 nm, as shown in Figure 8 (a). These large tubes were comparable to the ones located in STON12-RM800 in Figure 4 (f). STON8-RM800 produced nests of carbon nanotubes which are presented in Figure 8 (b, c), with a close-up in Figure 8 (d). The degradation of conversion could be related to the loss of effective catalyst due to the encapsulation by coking. When the particle size or the composition is not well-tuned, the high C-H cracking activity of Ni might produce more carbon on the surface than the it can

catalyze to form CNT.[39, 40] The well-controlled addition of precise metals or Cu to Ni in the future could suppress this process.[41]

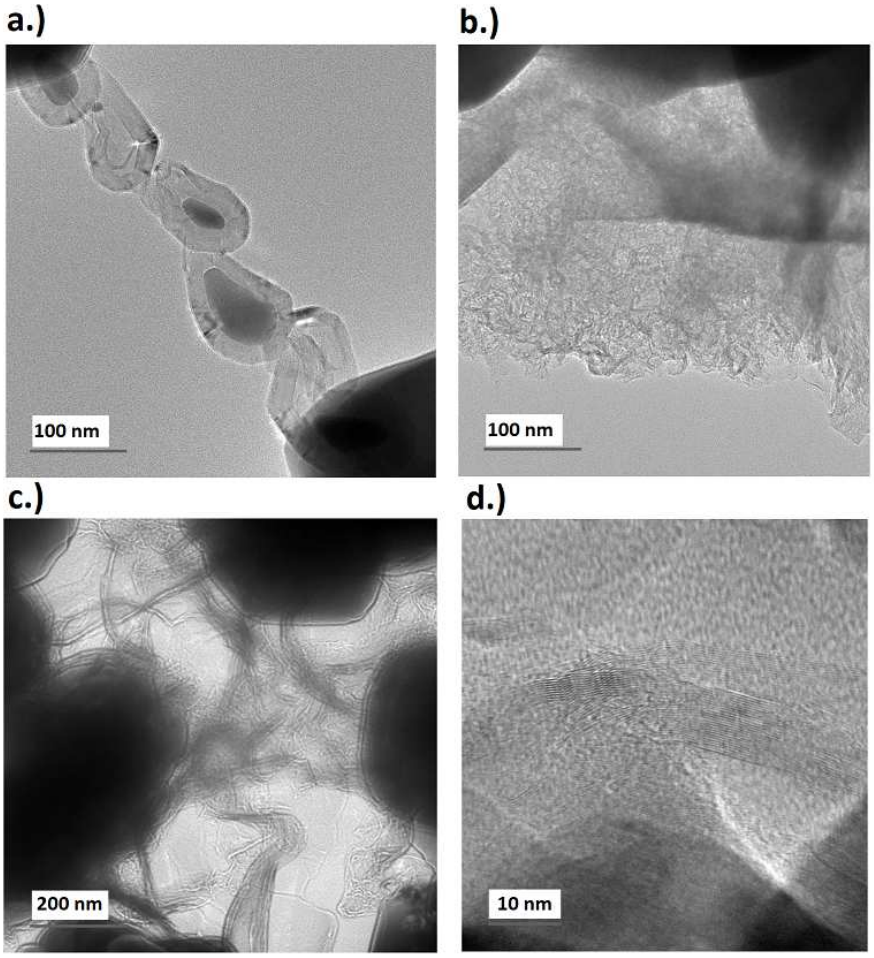

Figure 8. TEM photos of STON8-RM800. a.) A large bamboo structured fiber, b.) & c.) a cluster/nest of carbon formed, and d.) a close-up of a tube from the nest.

For the first time, carbon nanotubes were grown by us on an exsolution perovskite structure ceramic catalyst under microwave heating during methane decomposition. Between the two catalysts, STON8-RM800 had overall better methane conversion results, despite having a slightly lower initial methane conversion than STON12-RM800.

Figure 9 shows the Raman spectrum of CNTs produced by STON8-RM800. The produced carbon exhibits a D band at 1350 cm^{-1}, which corresponds to the disorder/defects from the walls or the open ends of the CNTs, and the G band at around 1590 cm^{-1}, which is the primary Raman-active mode of the sp2 bonded carbon present in a sheet configuration of graphite. The intensity ratio

between the D and G bands, I_D/I_G = 0.91, verifies that the produced CNTs are multi-walled, consistent with the TEM results.

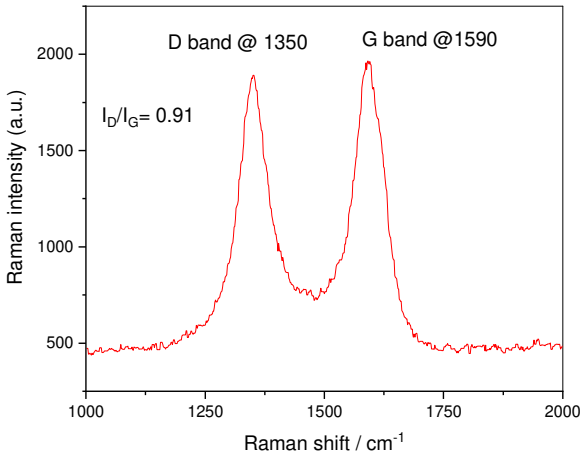

Figure 9. Raman spectrum of CNT produced by STON8-RM800

Microwave catalytic conversion is an emerging technology for efficiently converting chemicals into value-added products or environmentally benign species. However, due to the requirement of dielectric properties and competing side reactions, there are two major technical challenges in microwave pyrolysis: microwave responsiveness to generate enough temperature on the catalyst and stability towards the gas atmosphere, possibly causing temperature gradients in the catalyst. Along with recyclability and manufacturing scalability considerations, a significant portion of the transitional thermal catalysts are screened out, such as the most common SiO2, Al2O3, MgO series.[42, 43] To date, popular microwave catalysts for heterogeneous catalysis are still carbon-based materials due to their abundance and environmental benignity, as well as non-sinterability.[44] Precious metal carbon-based catalysts (e.g., Pt/C, Ru/C, etc.) have achieved superior performance in microwave methane conversion. In our previous study, the conversion rate of the 10Ni–1Pd/CNT catalyst yielded a 50% conversion after 320 minutes of operation.[30] However, the use of precious metals and the difficulty in recycling them urge us to explore more options through this study.

The value of this material in this study lies in its inherent ability to heat under microwave excitation and provide strong catalyst-base support for CNT growth during methane decomposition. STON's responsiveness to microwave provides a unique opportunity for

methane decomposition and CNT growth. High-temperature catalytic sites can be achieved at lower operating temperatures with the use of microwaves. When the benefits of microwave heating are paired with the flexibility of the perovskite structure, many opportunities arise for adaptable materials, regeneration of catalysts, and increased purity of CNTs through the method of inspiring base growth over tip growth. Continued development of promoters is needed to further enhance the methane conversion and selectiveness of the CNTs and to mitigate the degradation of the STON material system.

4. Conclusion

The study proved in concept the method of using a surface exsolving perovskite ceramic catalyst, nickel-doped strontium titanium oxide, to produce carbon nanotubes during methane decomposition under microwave heating. Various treatment compositions have been investigated. A 12h dwell time in hydrogen at 600°C proved to be superior. The optimal temperature discovered for the 12h dwell reduction was 800°C. Increasing temperature instead of Ni content tended to result in a more uniform size of the exsolve particle generated. $SrTiNi_{0.08}O_3$ (STON8) was the optimal Ni content for methane conversion and CNT generation using RM800. STON8-RM800 was tested at 500°C in a microwave reactor with an input gas of methane with a flow rate of 9 mL/min and nitrogen with a flow rate of 21 mL/min and had achieved a methane conversion rate of around 40% which levels to ~17% after two hours.

Notes

The authors declare no conflict of interest.

Acknowledgments

The authors acknowledge the financial support from the US Department of Energy under contract DE-FE-0031866. We acknowledge the use of the WVU Shared Research Facilities.

References

[1] Yoong Ahm Kim TH, Morinobu Endo, Mildred S. Dresselhaus. Springer Handbook of Nanomaterials 2013.

[2] Miao M, Liu T, Bai J, Wang Y. Engineering the wetting behavior of ceramic membrane by carbon nanotubes via a chemical vapor deposition technique. J Membr Sci. 2022;648:120357.

[3] Li Y, Wang J, He J, Zeng R, Miao M, Wang Y, et al. Carbon nanotubes@fly ash Janus composite membrane prepared from fly ash and waste plastics for efficient solar membrane distillation. J Membr Sci. 2023;672:121463.

[4] Pudukudy M, Yaakob Z, Takriff MS. Methane decomposition into COx free hydrogen and multiwalled carbon nanotubes over ceria, zirconia and lanthana supported nickel catalysts prepared via a facile solid state citrate fusion method. Energy Convers Manage. 2016;126:302-15.
[5] Pudukudy M, Yaakob Z, Dahani N, Takriff MS, Hassan NSM. Production of COx free hydrogen and nanocarbon via methane decomposition over unsupported porous nickel and iron catalysts. J Cluster Sci. 2017;28:1579-94.
[6] Pudukudy M, Yaakob Z, Kadier A, Takriff MS, Hassan NSM. One-pot sol–gel synthesis of Ni/TiO2 catalysts for methane decomposition into COx free hydrogen and multiwalled carbon nanotubes. Int J Hydrogen Energy. 2017;42:16495-513.
[7] Pudukudy M, Yaakob Z, Syahri KM, Jia Q, Shan S. Production of hydrogen-rich syngas and multiwalled carbon nanotubes by biogas decomposition over zirconia supported iron catalysts. Journal of Industrial and Engineering Chemistry. 2020;84:150-66.
[8] Pudukudy M, Kadier A, Yaakob Z, Takriff MS. Non-oxidative thermocatalytic decomposition of methane into COx free hydrogen and nanocarbon over unsupported porous NiO and Fe2O3 catalysts. Int J Hydrogen Energy. 2016;41:18509-21.
[9] Pudukudy M, Yaakob Z, Takriff MS. Methane decomposition over Pd promoted Ni/MgAl2O4 catalysts for the production of COx free hydrogen and multiwalled carbon nanotubes. Appl Surf Sci. 2015;356:1320-6.
[10] Pudukudy M, Yaakob Z, Jia Q, Takriff MS. Catalytic decomposition of undiluted methane into hydrogen and carbon nanotubes over Pt promoted Ni/CeO 2 catalysts. New J Chem. 2018;42:14843-56.
[11] Pudukudy M, Yaakob Z, Jia Q, Takriff MS. Catalytic decomposition of methane over rare earth metal (Ce and La) oxides supported iron catalysts. Appl Surf Sci. 2019;467:236-48.
[12] Pudukudy M, Yaakob Z, Mazuki MZ, Takriff MS, Jahaya SS. One-pot sol-gel synthesis of MgO nanoparticles supported nickel and iron catalysts for undiluted methane decomposition into COx free hydrogen and nanocarbon. Applied Catalysis B: Environmental. 2017;218:298-316.
[13] Pudukudy M, Yaakob Z. Methane decomposition over Ni, Co and Fe based monometallic catalysts supported on sol gel derived SiO2 microflakes. Chem Eng J. 2015;262:1009-21.
[14] Saraswat SK, Pant KK. Synthesis of hydrogen and carbon nanotubes over copper promoted Ni/SiO2 catalyst by thermocatalytic decomposition of methane. Journal of Natural Gas Science and Engineering. 2013;13:52-9.
[15] Abdullahi I, Sakulchaicharoen N, Herrera JE. A mechanistic study on the growth of multi-walled carbon nanotubes by methane decomposition over nickel–alumina catalyst. Diamond and Related Materials. 2012;23:76-82.
[16] Shen Y, Lua AC. Sol–gel synthesis of titanium oxide supported nickel catalysts for hydrogen and carbon production by methane decomposition. Journal of Power Sources. 2015;280:467-75.
[17] Manoy Pudukudy ZY, Mohd Zulhamizan Mazuki, Mohd Sobri Takriff, Seri Suriani Jahaya. One-pot sol-gel synthesis of MgO nanoparticles supported niickel and iron catalysts for undiluted methane decomposition into COx free hydrogen and nanocarbon. Applied Catalysis B, Environmental. 2017;218C:298-316.
[18] Kim M-J, Joo Park S, Duk Kim K, Kim W, Chan Nam S, Seok Go K, et al. Fabrication of carbon nanotube with high purity and crystallinity by methane decomposition over ceria-supported catalysts. Journal of Industrial and Engineering Chemistry. 2023;119:315-26.
[19] Dipu AL. Methane decomposition into COx-free hydrogen over a Ni-based catalyst: An overview. International Journal of Energy Research. 2021;45:9858-77.
[20] Park SJ, Kim K-D, Park YS, Go KS, Kim W, Kim M, et al. Effect of reduction conditions of Mo-Fe/MgO on the formation of carbon nanotube in catalytic methane decomposition. Journal of Industrial and Engineering Chemistry. 2022;109:384-96.

[21] E.T. Thisten T-WC. Microwave processing: fundementals and applications. Composites Part A: Applied Science and Manufacturing 1999;30:1055-71.
[22] Xunli Zhang DOH, and D. Michael P. Mingos. Effects of microwave dielectric heating on heterogeneous catalysts. Catalysis Letters 2003;88:33-8.
[23] Gangurde LS, Sturm GSJ, Valero-Romero MJ, Mallada R, Santamaria J, Stankiewicz AI, et al. Synthesis, characterization, and application of ruthenium-doped SrTiO 3 perovskite catalysts for microwave-assisted methane dry reforming. Chemical Engineering and Processing - Process Intensification. 2018;127:178-90.
[24] Ajmer Singh Grewal KK, S. Redhu, S. Bhardwaj Microwave assisted synthesis: a green chemistry approach. International Research Journal of Pharmaceutical and Applied Sciences 2013;3.5:278-85.
[25] Mello PA, Barin JS, Guarnieri RA. Microwave Heating. Microwave-Assisted Sample Preparation for Trace Element Analysis2014. p. 59-75.
[26] Sun J, Wang W, Yue Q. Review on Microwave-Matter Interaction Fundamentals and Efficient Microwave-Associated Heating Strategies. Materials (Basel). 2016;9.
[27] Zeng X, Fu D, Sheng H, Xie S, Li X, Hu Q, et al. Growth and morphology of carbon nanostructures by microwave-assisted pyrolysis of methane. Physica E: Low-dimensional Systems and Nanostructures. 2010;42:2103-8.
[28] Domínguez A, Fidalgo B, Fernández Y, Pis J, Menéndez J. Microwave-assisted catalytic decomposition of methane over activated carbon for CO2-free hydrogen production. International Journal of Hydrogen Energy. 2007;32:4792-9.
[29] Fidalgo B, Fernández Y, Zubizarreta L, Arenillas A, Domínguez A, Pis J, et al. Growth of nanofilaments on carbon-based materials from microwave-assisted decomposition of CH4. Applied Surface Science. 2008;254:3553-7.
[30] Jiang C, Wang IW, Bai X, Balyan S, Robinson B, Hu J, et al. Methane Catalytic Pyrolysis by Microwave and Thermal Heating over Carbon Nanotube-Supported Catalysts: Productivity, Kinetics, and Energy Efficiency. Ind Eng Chem Res. 2022;61:5080-92.
[31] Lindenthal L, Buchinger R, Drexler H, Schrenk F, Ruh T, Rameshan C. Exsolution Catalysts—Increasing Metal Efficiency. Encyclopedia. 2021;1:249-60.
[32] Otto S-K, Kousi K, Neagu D, Bekris L, Janek J, Metcalfe IS. Exsolved Nickel Nanoparticles Acting as Oxygen Storage Reservoirs and Active Sites for Redox CH4 Conversion. ACS Applied Energy Materials. 2019;2:7288-98.
[33] Park YS, Kang M, Byeon P, Chung S-Y, Nakayama T, Ko T, et al. Fabrication of a regenerable Ni supported NiO-MgO catalyst for methane steam reforming by exsolution. Journal of Power Sources. 2018;397:318-24.
[34] Meng X, Wang Y, Zhao Y, Zhang T, Yu N, Chen X, et al. In-situ exsolution of nanoparticles from Ni substituted Sr2Fe1.5Mo0.5O6 perovskite oxides with different Ni doping contents. Electrochimica Acta. 2020;348.
[35] Jia Q, Liu J, Zhong L, Li Y, Duan D. Preparation of the regular polyhedral single-crystalline SrTiO3 particles with exposing different crystal facets. Mater Lett. 2021;288:129338.
[36] Fabiola N. Aguero AMB, Maria Asuncion Fernandez, Lius E. Cadus Suface nickel particles generated by exsolution from a perovskite structure. Journal of Solid State Chemistry 2019;273:75-80.
[37] Meng X, Wang Y, Zhao Y, Zhang T, Yu N, Chen X, et al. In-situ exsolution of nanoparticles from Ni substituted Sr2Fe1.5Mo0.5O6 perovskite oxides with different Ni doping contents. Electrochim Acta. 2020;348:136351.
[38] Neagu D, Kyriakou V, Roiban I-L, Aouine M, Tang C, Caravaca A, et al. In situ observation of nanoparticle exsolution from perovskite oxides: from atomic scale mechanistic insight to nanostructure tailoring. ACS Nano. 2019;13:12996-3005.

[39] Msheik M, Rodat S, Abanades S. Methane cracking for hydrogen production: A review of catalytic and molten media pyrolysis. Energies. 2021;14:3107.
[40] Zhang C, Zhang W, Drewett NE, Wang X, Yoo SJ, Wang H, et al. Integrating catalysis of methane decomposition and electrocatalytic hydrogen evolution with Ni/CeO2 for improved hydrogen production efficiency. ChemSusChem. 2019;12:1000-10.
[41] Cazaña F, Afailal Z, González-Martín M, Sánchez JL, Latorre N, Romeo E, et al. Hydrogen and CNT Production by Methane Cracking Using Ni–Cu and Co–Cu Catalysts Supported on Argan-Derived Carbon. ChemEngineering. 2022;6:47.
[42] Fidalgo B, Arenillas A, Menéndez J. Mixtures of carbon and Ni/Al2O3 as catalysts for the microwave-assisted CO2 reforming of CH4. Fuel Process Technol. 2011;92:1531-6.
[43] Palma V, Barba D, Cortese M, Martino M, Renda S, Meloni E. Microwaves and heterogeneous catalysis: A review on selected catalytic processes. Catalysts. 2020;10:246.
[44] Nguyen HM, Sunarso J, Li C, Pham GH, Phan C, Liu S. Microwave-assisted catalytic methane reforming: A review. Applied Catalysis A: General. 2020;599:117620.